Chemical Physics Letters 476 (2009) 116–119

Contents lists available at ScienceDirect

Chemical Physics Letters

journal homepage: www.elsevier.com/locate/cplett

Solute order parameters in liquid crystals from NMR spectra solved with evolutionary algorithms: Application of double Maier–Saupe Kobayashi–McMillan theory

Adrian C.J. Weber [a], Xuan Yang [a], Ronald Y. Dong [b], W. Leo Meerts [c,d], E. Elliott Burnell [a,*]

[a] Chemistry Department, University of British Columbia, 2036 Main Mall, Vancouver, BC, Canada V6T 1Z1
[b] Department of Physics and Astronomy, University of British Columbia, 6224 Agricultural Rd, Vancouver, BC, Canada V6T 1Z1
[c] Molecular- and Biophysics Group, Institute for Molecules and Materials, Radboud University Nijmegen, P.O Box 9010, 6500 GL Nijmegen, The Netherlands
[d] Department of Physical Chemistry, Vrije Universiteit, De Boelelaan 1083, 1081 HV Amsterdam, The Netherlands

ARTICLE INFO

Article history:
Received 20 May 2009
In final form 2 June 2009
Available online 6 June 2009

ABSTRACT

We obtain dipolar couplings via a novel application of evolutionary algorithms solving for multiple spin-systems simultaneously and automatically from the NMR spectra of several solutes in several nematic and smectic liquid crystal solvents. The order parameters obtained from the dipolar couplings are used to test a novel Hamiltonian that includes two Maier–Saupe nematic terms plus Kobayashi–McMillan smectic A terms. It is shown that this Hamiltonian can rationalize the NMR experiments with physically reasonable smectic order parameters and Hamiltonian prefactors.

Two limits to the study of condensed matter by NMR are the ability to solve proton spectra and the availability of a Hamiltonian that describes the intermolecular interactions well. This is especially the case in the study of ordered fluids where the spectra of solute molecules are dominated by dipolar couplings [1]. The prospect of automated analysis of such spectra has been investigated with considerable success [2]. In later developments evolutionary algorithms (EAs) were found to yield solutions of moderately complicated molecules but often required operator intervention so as to avoid false minima [3,4]. A later application of the genetic algorithm proved to be more robust, avoiding false minima without operator intervention [5]. More recently the use of covariance matrix adaptation evolution strategy (CMA-ES) [6] has made it possible to solve very complicated spectra (such as oriented pentane with many of its roughly 20000 transitions overlapping) that would not have been otherwise possible by conventional means [7].

An interesting property of liquid crystals is the orientational ordering of molecules that make up the nematic phase and their positional ordering in the smectic A phase [8]. Nematic liquid crystals have uniaxial orientational order along an average direction called the director. For many purposes these molecules can be approximated by axially symmetric rods that would then have a single nematic order parameter S_L. If the nematic phase were to be perfectly ordered with all rods aligned along the director an S_L value of 1 is obtained whereas if it were heated up to the isotropic phase the S_L would become 0.

The smectic A phase has positional as well as orientational order. More specifically liquid crystal molecules will arrange, on average, into layers whose planes are perpendicular to the director. Kobayashi–McMillan theory provides a way to account for positional order with the use of additional order parameters [9,10]. One of these will be τ_L which is zero if the centres of molecules are spread evenly across layers (as in a nematic) and 1 if they occupy a single position in the centre of the layer. But S_L, the liquid crystal orientational order parameter, can change as the molecule goes deeper into the layer so there must be a nematic–smectic A coupling which will have an orientational–translational order parameter called κ_L. This theory has been applied in previous studies, one of which used Density Functional Theory methods for the solute–solvent potential [11]. It has also been used in the context of solutes as probes of the liquid crystal environment, but many assumptions were necessary. While the attempt was to test the Kobayashi–McMillan (KM) theory, the application was ironically hampered by an inadequate description of the nematic phase [12–14].

There is a wealth of literature dealing with the kinds of intermolecular forces that solutes experience when dissolved in liquid crystals [1,15–20]. There is still much disagreement as to which effects dominate the nematic potential. However, there is compelling evidence to support a large role for size and shape effects [15]. More recently it has been shown that the use of two independent

* Corresponding author. Fax: +1 604 822 2847.
E-mail addresses: adri@chem.ubc.ca (A.C.J. Weber), rondong@phas.ubc.ca (R.Y. Dong), leo.meerts@science.ru.nl (W. Leo Meerts), elliott.burnell@ubc.ca (E. Elliott Burnell).

0009-2614/$ - see front matter © 2009 Elsevier B.V. All rights reserved.
doi:10.1016/j.cplett.2009.06.002

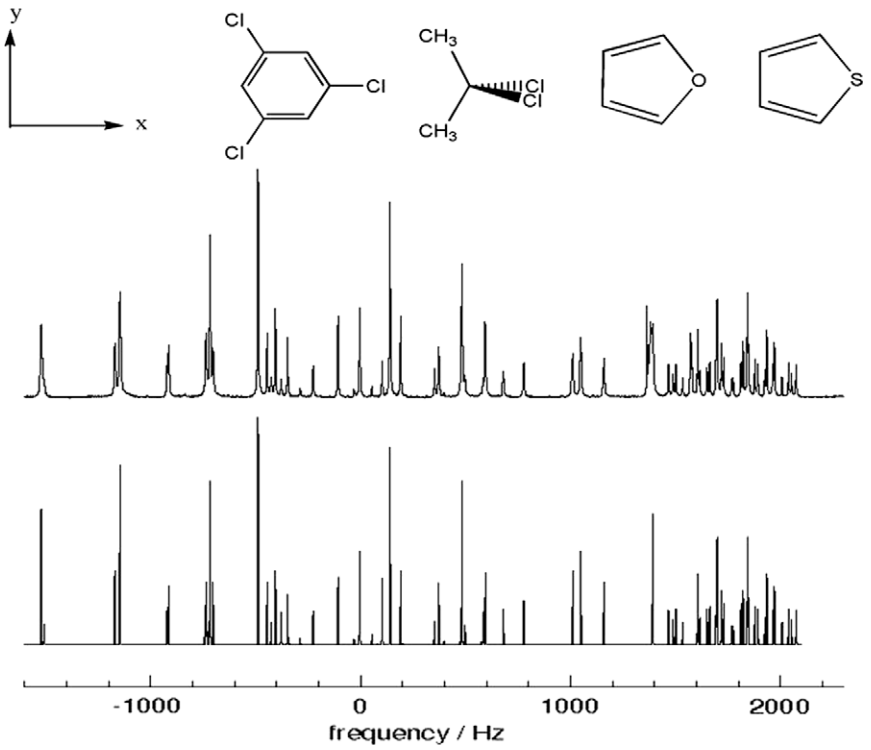

Fig. 1. The upper plot is of the experimental 400 MHz NMR spectrum while the lower is found using the CMA-ES. The peaks of the solutes (from left to right: tcb, clpro, fur and thio shown above in the molecule fixed coordinate system) are interspersed with one another.

mean-field Maier–Saupe terms (MSMS) in the nematic potential can fit experimental order parameters to better than 5% [21][1]. In what follows we utilize advances provided by CMA-ES in spectral analysis along with a physically reasonable Hamiltonian that combines the MSMS and KM theories to rationalize NMR observables of solutes dissolved in smectic and nematic phases.

The CMA-ES uses the principles of natural selection to evaluate potential solutions and the history of change in previous generations (a group of potential solutions) to guide a present generation towards a global minimum of an error surface. The solution at this minimum can be thought of as the NMR parameters (chemical shifts, scalar couplings and direct couplings) which best replicate the experimental NMR spectrum. First, an operator must choose reasonable upper and lower limits for each parameter. This will define the search or parameter space and one hopes that the correct solution is a point in this multidimensional space. A population of parameter sets are chosen randomly within the defined limits. Calculated spectra are generated from each member of the population and can be thought of as a vector **f** just as the list of intensities and frequencies of the experimental spectrum can be thought of as a vector **g**. Then by defining the Fitness function:

$$F_{fg} = \frac{(\mathbf{f}\cdot\mathbf{g})}{\|\mathbf{f}\|\|\mathbf{g}\|} \tag{1}$$

a number of the best parameter sets, with F_{fg} closest to 1, can be chosen as the next generation parents. This number is chosen by the operator and is typically 50% of the population size. A population will be created from these parents in a mutative step-size fashion. The offspring of this next generation will be spread out over a larger region of the parameter space due to the movement from selection in the previous generation. A new 'most fit' solution will be selected according to F_{fg} but the next parents location in parameter space will be a weighted sum of the last two movements. This memory effect of the evolutionary algorithm, which uses past mutation vectors coupled with natural selection to calculate the parents of a next generation, helps to overcome local minima and move closer to the global error minimum until convergence is reached. The CMA-ES approach was quite successful (see Fig. 1) in the current study of furan (fur), thiophene (thio), 2,2-dichloropropane (clpro) and 1,3,5-trichlorobenzene (tcb) dissolved in the liquid crystal 4-*n*-octyl-4′-cyanobiphenyl (8CB) that forms both a nematic and a lower temperature smectic A phase. While the spectra are not as congested as the spectrum of oriented pentane [7], the parameter space is still comparably large as there are four independent parameter sets. Specifically, the pentane parameter space was defined by 11 dipolar couplings (D_{ij}), 3 chemical shifts (ω_i) and 9 indirect couplings (J_{ij}) while that of the combined solutes is composed of 11 D_{ij}, 6 ω_i and 3 scaling parameters that scale the relative intensities of solutes. The result is impressive since all solutes are solved for simultaneously and automatically. This achievement will be crucial for future more elaborate studies of solutes in the nematic and smectic phases of a given liquid crystal.

All the solutes were dissolved in roughly equal amounts in 8CB for a total mole fraction of about 2% so that interactions amongst solutes can be ignored. It is important that solutes be dissolved in the same sample tube (as was done here) so that they experience the same environment. Spectra were collected in 0.5 or 1 K steps on both sides of the nematic–smectic A transition. The resulting dipolar couplings obtained from CMA-ES analysis were then used to calculate solute order parameters using a modified version of the computer program SHAPE [22] and structures from the literature [23–26]. One can see that the order parameters are affected by the smectic environment when plotting the solute order tensor asymmetry

$$R = (S_{xx} - S_{yy})/S_{zz} \tag{2}$$

[1] Note that the S_{xx} values for fluorobenzene in 1132 and MM reported in Table 1 of Ref. [21] should both be positive.

versus solute S_{xx} and noting the change in slope at the phase transition as shown in Fig. 2.

The MSMS nematic potential for solutes with two or fewer independent order parameters can be written as:

$$H_{N,Ls}(\Omega_s) = -\frac{3}{4}\sum_{i=1}^{2} G_{L,ZZ}(i)\beta_{s,zz}(i) \times \left[\left(\frac{3}{2}\cos^2(\theta_s) - \frac{1}{2}\right) + \frac{b_s(i)}{2}\sin^2(\theta_s)\cos(2\phi_s)\right] = H_{MS_1} + H_{MS_2}, \quad (3)$$

where

$$b_s(i) = \frac{\beta_{s,xx}(i) - \beta_{s,yy}(i)}{\beta_{s,zz}(i)}. \quad (4)$$

Consistent with Maier–Saupe theory, the $G_{L,ZZ}(1)$ and $G_{L,ZZ}(2)$ are taken to be mean-field properties of the liquid crystal that interact with some solute properties which are denoted by the $\beta_{s,\gamma\gamma}(1)$ and $\beta_{s,\gamma\gamma}(2)$. The index γ runs over the molecule fixed x, y and z axes. Given the assumptions made in previous studies using Kobayashi–McMillan theory [12–14] and the recent success of the MSMS potential in dealing with nematics, the Hamiltonian for the potential in a smectic liquid crystal is proposed to be:

$$H_{A,Ls}(\Omega_s, Z) = H_{MS_1}\left(1 + \kappa'_L(1)\cos\left(\frac{2\pi Z}{d}\right)\right) + H_{MS_2}\left(1 + \kappa'_L(2)\cos\left(\frac{2\pi Z}{d}\right)\right) - \tau'_{Ls}\cos\left(\frac{2\pi Z}{d}\right), \quad (5)$$

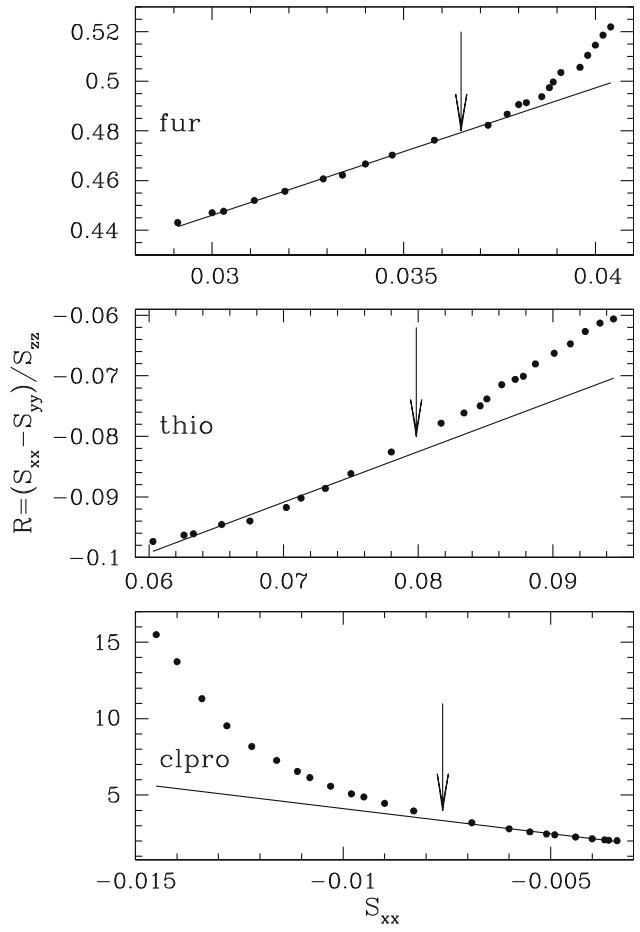

Fig. 2. The asymmetry in the order parameters (R) for fur, thio and clpro are plotted against their respective S_{xx}. An arrow marks the phase transition and the lines are the best fit to the points in the nematic phase.

where $\kappa'_L(1)$ and $\kappa'_L(2)$ are the nematic–smectic coupling Hamiltonian prefactors, one to modulate each of the two nematic ordering mechanisms as we move across a layer, and it is reasonable to take them as a liquid crystal property. There is one τ'_{Ls} (the solute smectic prefactor) for each solute in a given liquid crystal and d is the width of the layer while Z ($Z = 0$ in the centre of a layer) maps the direction parallel to the director which lies along the magnetic field direction in the experiments reported here.

Because the $\beta_{s,\gamma\gamma}(i)$ are solute properties, and hence not functions of temperature or liquid crystal solvent, their values are first obtained by fitting to order parameters of several molecules (including the ones of interest) in five different nematic liquid crystals with the MSMS potential. In particular we have used the liquid crystals: Merck ZLI-1132 (1132), a 'magic mixture' of 55 wt% 1132 and 45 wt% *p*-ethoxybenzylidene-*p*′-*n*-butylaniline (EBBA), EBBA and both 8CB and 4-*n*-octyloxy-4′-cyanobiphenyl (8OCB) at three different temperatures spanning the nematic phase. The analysis is carried out in the same manner as in [21] using the relationship:

$$S_{s,\gamma\gamma} = \frac{\int d\Omega_s\left(\frac{3}{2}\cos^2(\theta_{s,\gamma}) - \frac{1}{2}\right)e^{\frac{-H_{N,Ls}(\Omega_s)}{k_BT}}}{\int d\Omega_s e^{\frac{-H_{N,Ls}(\Omega_s)}{k_BT}}}. \quad (6)$$

With the $\beta_{s,\gamma\gamma}(i)$'s now fixed we proceed by fitting the experimental order parameters for the solutes of interest at each temperature in both the nematic and smectic phases of 8CB, using the nematic potential only by varying $G_{L,ZZ}(1)$ and $G_{L,ZZ}(2)$, and notice that the RMS of the fit increases significantly in the smectic phase (open circles in inset to Fig. 3). We then attempt to fit the $S_{s,\gamma\gamma}$ in the smectic A phase to the combined MSMS-KM Hamiltonian of Eq. (5) varying all free parameters ($G_{L,ZZ}(i)$, $\kappa'_L(i)$ and τ'_{Ls}) with the expression:

$$S_{s,\gamma\gamma} = \frac{\int d\Omega_s \int_0^d \left(\frac{3}{2}\cos^2(\theta_{s,\gamma}) - \frac{1}{2}\right)e^{\frac{-H_{A,Ls}(\Omega_s,Z)}{k_BT}}dZ}{\int d\Omega_s \int_0^d e^{\frac{-H_{A,Ls}(\Omega_s,Z)}{k_BT}}dZ} \quad (7)$$

to find that it does not converge and so are forced to make an assumption. In previous work, in order to be over-determined so

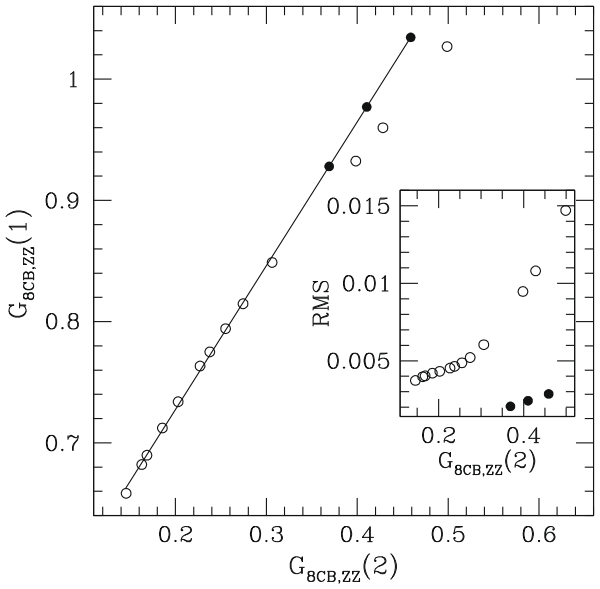

Fig. 3. $G_{8CB,ZZ}(1)$ is plotted against $G_{8CB,ZZ}(2)$ where the black points signify the use of the smectic Hamiltonian and the open points are obtained with the nematic potential only. The 10 points closest to the origin are from measurements in the nematic phase while the rest are in the smectic phase. *Inset*: The RMS of fits to either potential in both phases are plotted against $G_{8CB,ZZ}(2)$.

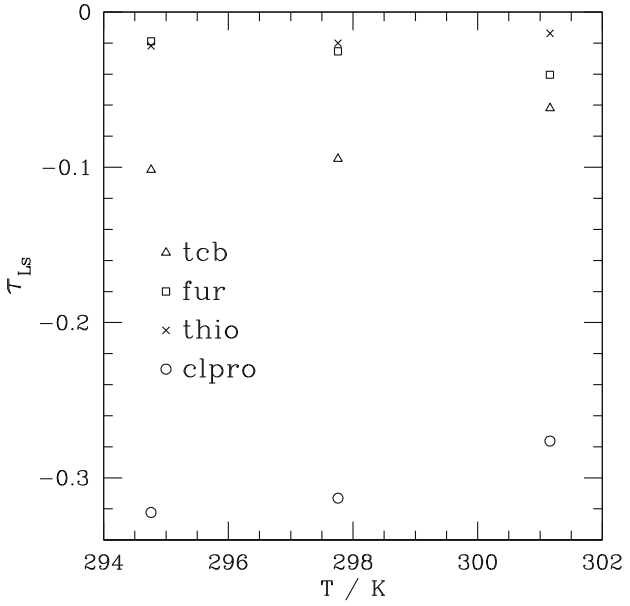

Fig. 4. The smectic order parameters τ_{Ls} are plotted against temperature for each of the solutes tcb, fur, thio and clpro.

as to solve for smectic Hamiltonian prefactors, we linearly extrapolated the interaction energy from the nematic into the smectic phase once for each solute (where some solutes showed some curvature) and used the extrapolation to estimate the smectic effect. This crude assumption has been circumvented by the MSMS theory. Here we make the single assumption that $G_{L,ZZ}(1)$ is linearly related to $G_{L,ZZ}(2)$. Hence, we extrapolate once for the liquid crystal by drawing a line through the nematic points of $G_{L,ZZ}(1)$ versus $G_{L,ZZ}(2)$ and forcing this relationship into the smectic phase as seen in Fig. 3. Under these circumstances we now vary $G_{L,ZZ}(2)$ (from which $G_{L,ZZ}(1)$ is calculated), $\kappa'_L(1)$ and $\kappa'_L(2)$ for the liquid crystal and a τ'_{Ls} for each solute to find that we obtain excellent fits (see inset of Fig. 3).

With the smectic Hamiltonian in hand we go on to calculate the solute smectic order parameters τ_{Ls} using:

$$\tau_{Ls} = \frac{\int d\Omega_s \int_0^d \cos\left(\frac{2\pi Z}{d}\right) e^{\frac{-H_{A,Ls}(\Omega_S,Z)}{k_B T}} dZ}{\int d\Omega_s \int_0^d e^{\frac{-H_{A,Ls}(\Omega_S,Z)}{k_B T}} dZ} \tag{8}$$

the results of which are shown in Fig. 4. The overall trend is satisfying in that the magnitude of τ_{Ls} (with the exception of fur) becomes smaller with increasing temperature as would be expected when approaching the nematic phase. A negative value of τ_{Ls} implies a preference for the interlayer region while a positive value indicates a preference to the centre of a layer. The closer the τ_{Ls} of either sign is to zero the less pronounced is its partitioning, with $\tau_{Ls} = 0$ meaning positional isotropy. It is interesting to note that clpro has the largest negative τ_{Ls} which means it displays the most partitioning to the interlayer region, as expected because the size and shape of clpro is fairly well approximated by a sphere. Fur and thio show less partitioning, but exhibit opposite trends with changing temperature. In particular fur tends to partition more to the interlayer region upon increasing temperature.

Turning now to the liquid crystal prefactors we note that the $G_{L,ZZ}(2)$ calculated with the smectic potential of Eq. (5) is smaller than that calculated with only the MSMS nematic potential of Eq. (3) for fits in the smectic phase as seen in Fig. 3. This shows that the nematic potential was accounting for the extra order of the smectic phase which was later picked up in a more appropriate way in the smectic potential. We obtain a $\kappa'_L(1)$ value of 0.38 which is constant and in good agreement with our previous studies. However, previously we had only one coupling prefactor which modulated all nematic mechanisms that were brought together as one term. With these restrictions now relaxed it is interesting to find a constant $\kappa'_L(2)$ value of -2.5, greater than 1 in absolute value. In other words, the second MS mechanism in Eq. (5) undergoes a sign change as a function of Z due to the nematic–smectic coupling in 8CB. This seems to imply that there are planes along Z where the second MS mechanism imposes no order and that there would be isotropy here were it not for the dominance of the first MS mechanism.

In summary, we have shown that an MSMS-KM potential can be used to obtain valuable information on solutes in the smectic phase in addition to some clues regarding the phase itself. These matters clearly merit further, more elaborate investigation which are much more manageable now that we can quickly solve spectra of multiple solutes automatically and simultaneously in liquid crystals using evolutionary algorithms.

References

[1] E.E. Burnell, C.A. de Lange (Eds.), NMR of Ordered Liquids, Kluwer Academic, Dordrecht, 2003.
[2] F. Castiglione, G. Celebre, G. De Luca, M. Longeri, J. Magn. Reson. 142 (2000) 216. and references therein.
[3] H. Takeuchi, K. Inoue, Y. Ando, S. Konaka, Chem. Lett. 11 (2000) 1300.
[4] K. Inoue, H. Takeuchi, S. Konaka, J. Phys. Chem. A 105 (2001) 6711.
[5] W.L. Meerts, C.A. de Lange, A.C.J. Weber, E.E. Burnell, Chem. Phys. Lett. 441 (2007) 342.
[6] N. Hansen, A. Ostermeier, Evolut. Comput. 9 (2) (2001) 159.
[7] W.L. Meerts, C.A. de Lange, A.C.J. Weber, E.E. Burnell, J. Chem. Phys. 130 (2009) 044504.
[8] R.Y. Dong, Nuclear Magnetic Resonance of Liquid Crystals, first edn., Springer-Verlag, New York, 1994.
[9] K.K. Kobayashi, Mol. Cryst. Liq. Cryst. 13 (1971) 137.
[10] W.L. McMillan, Phys. Rev. A 4 (1971) 1238.
[11] G. Celebre, G. Cinacchi, G. De Luca, J. Chem. Phys. 129 (2008) 094509.
[12] A. Yethiraj, Z. Sun, R.Y. Dong, E.E. Burnell, Chem. Phys. Lett. 398 (2004) 517.
[13] A. Yethiraj, A.C.J. Weber, R.Y. Dong, E.E. Burnell, J. Phys. Chem. B 111 (2007) 1632.
[14] A. Yethiraj, E.E. Burnell, R.Y. Dong, Chem. Phys. Lett. 441 (2007) 245.
[15] E.E. Burnell, C.A. de Lange, Chem. Rev. (Washington, DC) 98 (1998) 2359. and references therein.
[16] A. di Matteo, A. Ferrarini, G.J. Moro, J. Phys. Chem. B 104 (2000) 7764.
[17] A. Ferrarini, G.J. Moro, J. Chem. Phys. 114 (2001) 596.
[18] A. di Matteo, A. Ferrarini, J. Phys. Chem. B 105 (2001) 2837.
[19] G. Celebre, G. De Luca, Chem. Phys. Lett. 368 (2003) 359.
[20] G. Celebre, J. Phys. Chem. B 111 (2007) 2565.
[21] E.E. Burnell, L.C. ter Beek, Z. Sun, J. Chem. Phys. 128 (2008) 164901.
[22] P. Diehl, P.M. Heinrichs, W. Niederberger, Mol. Phys. 20 (1971) 139.
[23] B. Bak, D. Christensen, W.B. Dixon, L. Hansen-Nygaard, J. Rastrup-Andersen, M. Schottlander, J. Mol. Spectrosc. 9 (1962) 124.
[24] B. Bak, D. Christensen, L. Hansen-Nygaard, J. Rastrup-Andersen, J. Mol. Spectrosc. 7 (1961) 58.
[25] A. Almenningen, I. Hargittai, J. Brunvoll, A. Domenicano, S. Samdal, J. Mol. Struct. 116 (1984) 199.
[26] M. Hirota, T. Iijima, M. Kimura, Bull. Chem. Soc. Jpn. 51 (1978) 1589.